CONF-830605--8-Pt.2

DOE/ER/10361--4-Pt.2

DE86 006395

24th U.S. Symposium
on Rock Mechanics
June 1983

PART II

MODIFICATION OF FRACTURE SURFACES BY DISSOLUTION

BRANN JOHNSON
Center for Tectonophysics
and
Departments of Geology and Geophysics
Texas A&M University
College Station, TX 77843

ABSTRACT

This study focuses upon how and to what extent dissolution related fluid/rock interactions modify the morphology and roughness of surfaces on Sioux Quartzite. Dissolution experiments consisted of reacting small discs of Sioux Quartzite in sealed gold capsules containing either distilled water or 0.05 N to 4.0 N aqueous solutions of Na_2CO_3. *Samples were reacted at 200°C and 20 to 30 MPa fluid pressures for 2 to 5 days. Two markedly different starting surface textures were used: polished, optically flat surfaces and tensile fracture surfaces. An exploratory experiment also was performed to assess the occurrence of a pressure solution phenomenon on a polished quartzite surface at contact regions of indenting quartz sand grains.*

Scanning electron microscopy studies indicate progressive increases in the amount of dissolution produced significant changes of surface roughness for both initial surface textures. Surface roughness increased measureably, with the initially polished surfaces exhibiting the more dramatic changes. Intragranular and intergranular (grain boundary) cracks, pores and tubules play a dominant role in the evolution of surface roughness during dissolution. Crystallographic controls primarily affect the geometric form of dissolution features as a consequence of differing rates of dissolution with different crystallographic directions. Grain boundary widening, one of the more significant changes, is influenced also by this crystallographic control. In addition to dissolution fluid/rock interactions, a small amount of the secondary mineral, analcite, formed. More specifically, grain boundaries widened from an initial width of 0.1 to 1.0 μm to up to 30 μm for the more extensive dissolution; this grain boundary widening extended from one to two grain diameters inward from the original surface. The experiments clearly show that grinding and polishing induced microcracks influence the early stage of the changes of surface morphology and that one must give careful consideration of their influence when performing permeability experiments on "artificial" fracture surfaces (e.g., saw cuts) in a chemically reactive fluid environment.

The pressure solution experiments did not produce definitive results, but several surface features are suggestive of dissolution enhancement at load carrying contacts.

MASTER

DISTRIBUTION OF THIS DOCUMENT IS UNLIMITED

DISCLAIMER

This report was prepared as an account of work sponsored by an agency of the United States Government. Neither the United States Government nor any agency Thereof, nor any of their employees, makes any warranty, express or implied, or assumes any legal liability or responsibility for the accuracy, completeness, or usefulness of any information, apparatus, product, or process disclosed, or represents that its use would not infringe privately owned rights. Reference herein to any specific commercial product, process, or service by trade name, trademark, manufacturer, or otherwise does not necessarily constitute or imply its endorsement, recommendation, or favoring by the United States Government or any agency thereof. The views and opinions of authors expressed herein do not necessarily state or reflect those of the United States Government or any agency thereof.

DISCLAIMER

Portions of this document may be illegible in electronic image products. Images are produced from the best available original document.

INTRODUCTION

Flow of hot, aqueous fluids through fractured rock occurs in a number of natural and man initiated thermal-convective, circulation systems of geologic and engineering significance. As a consequence of water/rock interactions, the character of fracture-surface asperities and interasperity pore space can change with time and hence modify the fracture's effective hydraulic aperture and mechanical compliance. Water/rock interactions can result in dissolution of fracture asperities and, in some instances, formation of secondary minerals within interasperity pore space, either by metasomatic reactions or by crystallization from solution. The specific water/rock reactions and associated products are a function of the initial rock mineralogy and fluid composition, as well as fluid temperature and pressure. The dearth of experimental data on fracture permeability at elevated temperatures, however, does not allow one, presently, to predict for a given geologic situation whether the water/rock interactions will increase or decrease fracture permeability.

Research is currently in progress to help resolve this important problem. The long-term objective of our research is to measure and understand the variation of fracture permeability in several geologically significant rocks as a function of hydrothermal reaction with through-flowing aqueous fluids (H_2O, alkaline solutions, NaCl, sea water) at temperatures to 300°C, fluid pressures to 30 MPa and effective pressures to 70 MPa. The experiments are designed to evaluate the relative importance of dissolution reactions and secondary mineral formation upon changes of fracture permeability.

The elevated-temperature, corrosive fluid, permeability system is nearing completion. The first experiments will focus on assessing the roles of dissolution and pressure solution upon fracture permeability; the effects of secondary mineral formation will be studied in later experiments. Consequently, we have chosen to study the variation of the fracture permeability of a quartzite. As a preliminary to these planned experiments, several complementary studies have been undertaken: (1) experimental study of the evolution stages of a surface on Sioux Quartzite undergoing dissolution, with specific emphasis on the changes of surface roughness and asperity shape, and (2) an exploratory experiment to assess whether measureable pressure solution can occur within time constraints of a permeability experiment. The objective of the dissolution experiments is to provide a physical picture of the dissolution processes and identification of the important parameters affecting dissolution modification of fracture surface morphology. These studies will allow us to better interpret the results of the permeability experiment and provide the foundation for development of a theoretical model of permeability changes associated with dissolution reactions. Preliminary results of these experiments are presented below.

STARTING MATERIAL AND METHODS

Rock Material

The Sioux Quartzite is a low porosity (0.2-0.4%), medium grained (ca. 0.1 - 1.0mm), sedimentary rock composed predominately (> 99%) of tightly packed, subrounded to rounded detrital quartz grains with crystallographically continuous quartz overgrowths. Samples for this study come from the same block used by Friedman and Bur (1974), Johnson et al (1978), and Friedman and Johnson (1978): This block was provided by the Bureau of Mines and is part of their standard rock suite for rapid excavation (Krech et al, 1974). Previous studies (Friedman and Bur, 1974) indicate the Sioux Quartzite has: (1) a measureable residual strain, (2) no preferred orientation of crystallographic c-axes, (3) all grains contain healed, intragranular microfractures, (4) many grains exhibit undulose extinction (across entire grain including overgrowths), (5) deformation lamellae (planar concentrations of dislocations) are common and exhibit a preferred orientation, lying within 30° of the bedding plane and (6) grain boundaries significantly influence the propagation path of macroscopic tensile fractures (transgranular to intergranular fracture ratios are about 2). Bulk chemical analyses indicate the rock contains 0.04% Fe_2O_3 and 0.2% ± 0.1% Al_2O_3. The iron oxide occurs predominantly as small (submicron) bleds and rods of hematite usually concentrated at original detrital grain boundaries or along healed microfractures, but it also occurs as scattered inclusions within the quartz grains, as does tourmaline, zircon and rutile. The Al_2O_3 appears to be associated predominately with a small amount of kaolinite occurring at grain boundaries and within the overgrowths. SEM examination of fractured grains and polished surfaces reveal many grains contain holes or tubules of 1 μm or less in diameter (Fig. 1), sometimes exhibiting linear arrays. They are interpreted to be associated with healed microfractures and are analogous to microtubules reported by Shirey et al (1980) in plagioclase. Grain boundaries are often surfaces of weakness and

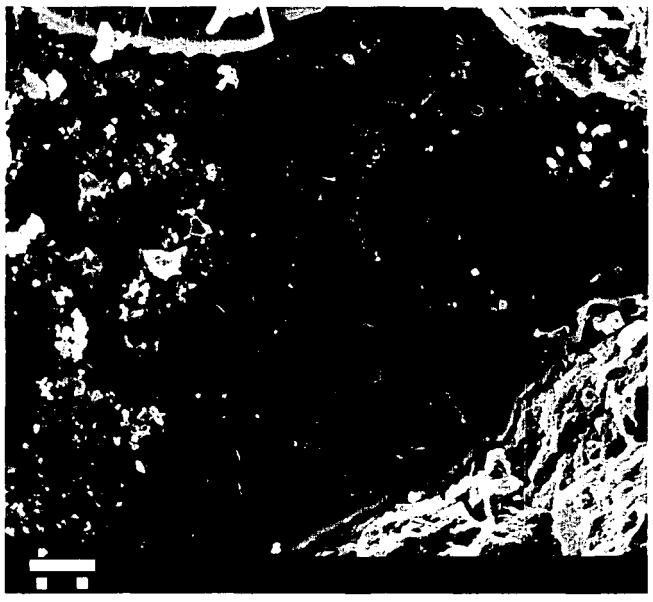

Figure 1. SEM photograph of transgranular fracture surface that intersects a number of intragranualr pores and tubules. Scale bar is 10 μm.

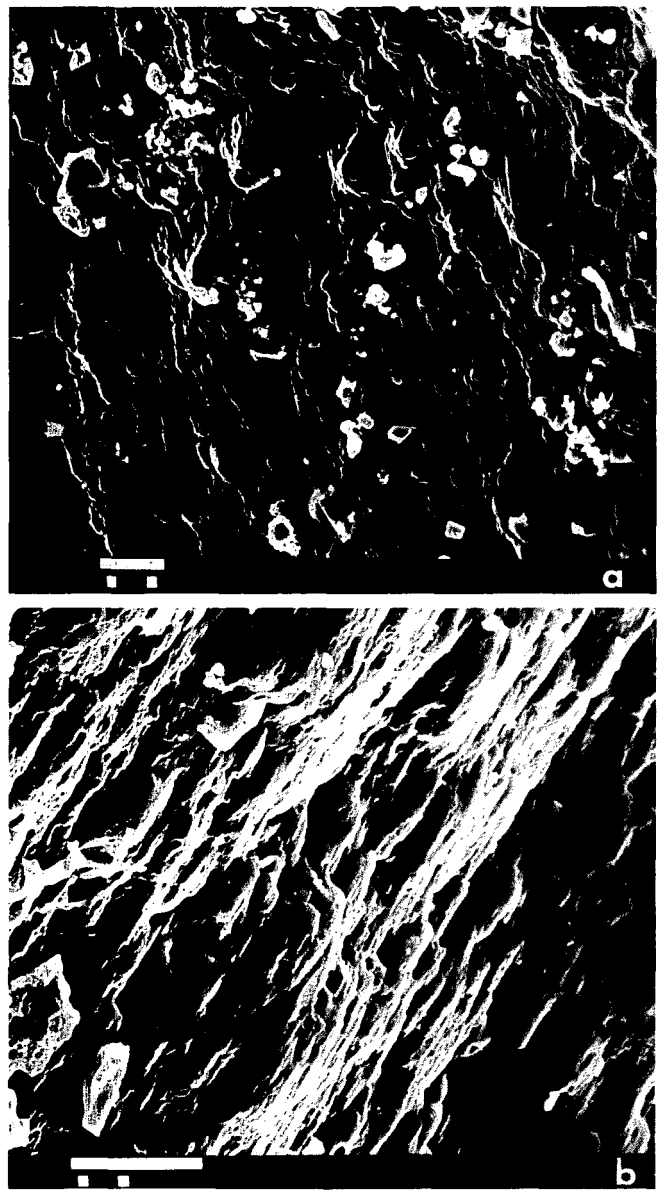

Figure 2. SEM photographs of representative grain boundary surfaces showing significant microroughness. Scale bar is 10 μm.

SEM indicates they typically have a significant microroughness (Fig. 2a) often exhibiting a crystallographically controlled surface texture (Figure 2b); holes or tubules appear to be common at grain boundaries.

Experiment and Observation Methods

Dissolution Experiments

The dissolution experiments consist of reacting, in a cold-seal hydrothermal reaction vessel, small discs (7.4 mm diameter x 3 to 5 mm thick, ca. 0.35 to 0.45 gm) of Sioux Quartzite in sealed gold capsules containing between 2 to 4 ml of either distilled water or a 0.05 to 4.0 N aqueous solution of Na_2CO_3. The Na_2CO_3 provides a buttered high pH solution that increases the solubility of quartz; solubility is proportional to the Na_2CO_3 concentration, hence we are able to obtain differing amounts of dissolution by varying the initial concentration. Experiments are conducted at 200°C and 20 to 30 MPa fluid pressure using a closed system, hydrothermal reaction vessel. Run times range from 2 to 5 days, which is sufficient for the fluid to closely approach saturation with respect to quartz. Quench of samples takes less than 1 hour with capsules being opening immediately. Fluid samples are recovered for chemical analysis and the sample is dried and weight loss determined. Documentation of change of surface morphology with varying amounts of dissolution is by means of scanning electron microscopy.

We have used two markedly different starting surface textures: polished, optically flat surfaces and tensile fracture surfaces. In both cases discs are obtained from segments of cores diamond core drilled parallel to bedding. For polished surfaces, the core is cut into thin discs and one surface progressively ground with SiC to 1000 grit, then diamond paste polished and finished with 0.3 μm alumina. Tensile fracture surfaces are prepared by three-point bending of cores.

Pressure Solution Experiments

A monolayer of subrounded to rounded quartz sand grains (ca. 100 μm diameter) was sandwiched between ends of two, polished, optically flat, cylinders of Sioux Quartzite. The sample, saturated with distilled water, was sustained under a triaxial load at 300°C for 4 days. Confining pressure, pore fluid pressure and axial load were adjusted to obtain a 10 to 15 MPa effective normal stress across the layer. During the experiment, loading column length and acoustic emissions were monitored continuously;the latter was monitored so as to allow adjustment of axial load to as high as possible without extensive fracture of the sand grains. Upon completion of the experiment, it was planned to examine with SEM the sand grains and the quartzite surfaces for evidence that pressure solution had occurred. Unfortunately, we lost confining pressure during the fourth day and a large number of grains were crushed. Consequently, only the polished, quartzite end pistons provide surfaces adequate for SEM examination.

RESULTS

Dissolution Studies

Progressive increases in the amount of dissolution produced significant changes of surface roughness for both initial surface textures. Surface roughness increased measurably, with the initially polished surfaces exhibiting the more dramatic changes. Intragranular and intergranular (grain boundary) cracks, holes and tubules play a dominant role in the evolution of surface roughness during dissolution. Crystallographic controls primarily affect the geometric form of dissolution features as a consequence of differing rates of dissolution with different crystallographic directions. Grain boundary widening, one of the more significant changes, is influenced also by this crystallographic control. In addition to dissolution fluid/rock interactions, a small amount of secondary mineral formation occurred. Below are presented the specifics of the results. First, for the polished, flat surfaces, then for the tensile fracture surfaces. The former clearly demonstrate the typical changes of roughness and allows identification of the important parameters. These experiments also clearly show how preparation of a "fracture" surface can potentially have a significant effect on the results of a permeability experiment entailing fluid/rock interactions.

Polished, Flat Surfaces

Figure 3 shows representative SEM overviews of surfaces of samples reacted in distilled water and 0.1N, 0.4N, and 4.0N Na_2CO_3 solutions. Table 1 provides some specific information for each sample, such as sample weight, percent weight loss, fluid volume, and duration of run; note, all experiments were performed at 200°C. Figure 3 and Table 1 show significant dissolution occurs as demonstrated by surface morphology changes and weight losses. Excepting the distilled water run, weight losses are approximately two times greater than predicted for dissolution alone. The increased weight loss reflects detachment of grains and grain segments as a consequence of dissolution at grain boundaries and long intragranular cracks. Sites of detached grains are indicated by the letter A in Fig. 3b, c, and d.

In addition to dissolution, a small amount (1 to 2%) of the zeolite, analcite, $Na(AlSi_2O_6) \cdot H_2O$, forms as a secondary mineral, as seen in Figure 3b and d (the trapezohedrons). This mineral typically has a hydrothermal association. It is believed the aluminum is coming from the small amount of kaolinite occurring at grain boundaries and within overgrowths. The amount of analcite formed is consistent with the Al_2O_3 content of the rock.

Examination of Figure 3a shows that dissolution in distilled water has highlighted grinding/polishing scratches and grain boundaries. The scratches typically consist of a series of closely spaced microcracks. The average secondary electron emission of the SEM picture varies from grain to grain as indicated by the differing "brightness" of the grains; this reflects differences of microroughness. Closer inspection (Figure 4a and b) shows numerous, small, closely spaced microcracks that have been widened by dissolution. These are predominantly grinding/polishing induced cracks. They range from 1 μm to 10 μm in length, with a spacing that is closely related to their crack length, i.e. the shorter cracks are more closely spaced. Dissolution has widened these cracks to between 0.1 to 0.5 μm. Furthermore, these microcracks often exhibit a preferred orientation that is interpreted to reflect the cleavage directions of quartz (typically $\{10\bar{1}1\}$, $\{01\bar{1}1\}$, and $\{10\bar{1}0\}$). In addition to the numerous microcracks, many grains exhibit small (0.1 - 0.7 μm diameter), elongate mounds or " pimples", often with their axes inclined at an uniform orientation across a single grain (Figure 4a and b); their orientation changes from grain to grain. This

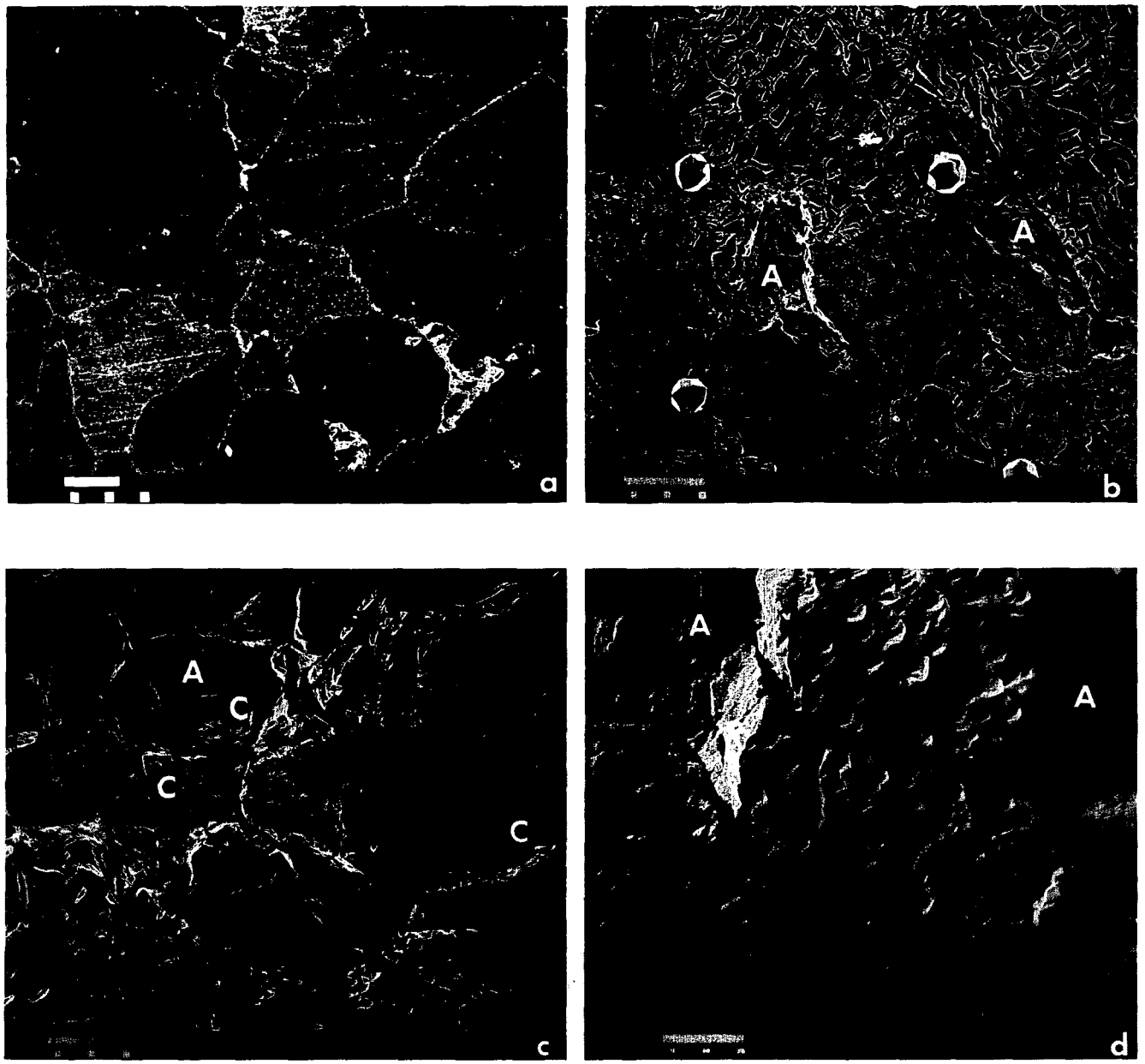

Figure 3. SEM photographs showing progressive modification of surface morphology with increasing amounts of dissolution. Initial surface is polished, optically flat. Scale bar is 100 μm. a) 4 ml distilled water; b) 4 ml 0.1N Na_2CO_3, secondary mineral is analcite; c) 4ml 0.4N Na_2CO_3; d) 4 ml 4.0 N Na_2CO_3.

TABLE 1

Sample ID	Surface Type	Initial Sample Wt. (gm)	Wt. Loss (%)	Fluid Volume (ml)	Na_2CO_3 (Normality)	Run Duration (days)
SQ-5	Polished	0.37041	0.66*	4	0	3
SQ-4	"	0.37524	2.54	4	0.1	3
SQ-3	"	0.37643	8.13	4	0.4	3
SQ-2	"	0.37223	15.09	4	0.4	3
SQ-1	"	0.36459	10.4	4	1.0	2
SQ-6	Fracture	0.43234	0.14	4	4.0	2
SQ-7	"	0.44863	2.24	4	0.1	2
SQ-8	"	0.48964	6.07	4	0.4	2
SQ-9	"	0.41907	12.34	4	4.0	2
SQ-10	"	0.37655	46.11	4	4.0	2
SQ-11	"	0.43980	0.71	3	0.05	5
SQ-12	"	0.43307	2.23	4	0.2	5
SQ-13	"	0.37109	3.98	3	0.4	5
SQ-14	"	0.38449	6.62	2	0.7	5
SQ-15	"	0.37551	6.80	2	1.0	5

1 all runs 200°C

* suspected capsule leak (confining pressure fluid is water) hence more extensive dissolution than normally expected for 4ml initial fluid volume.

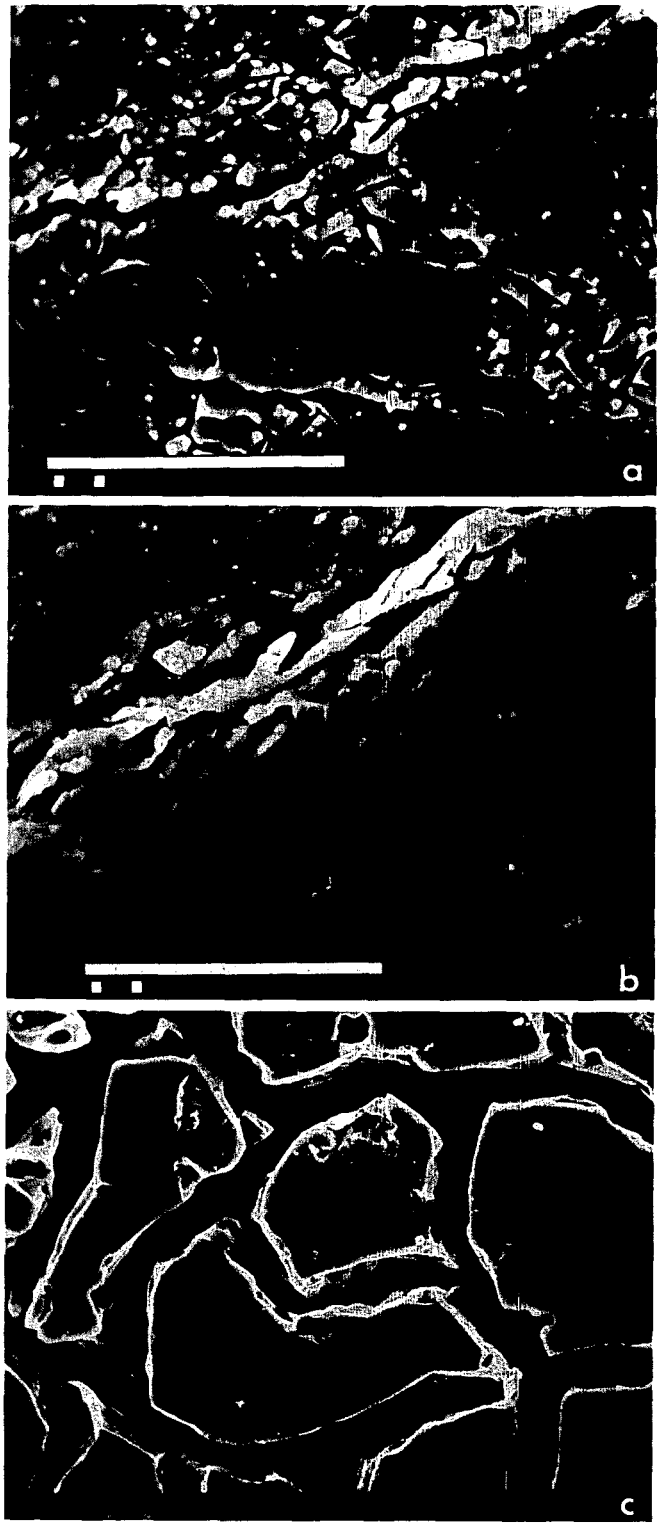

Figure 4. Small scale surface structures and dissolution features. Scale bar is 10 μm. a) and b) distilled water, each shows two grains with differing crystallographic orientations; c) 0.1 N Na_2CO_3, small cracks and "pimples" seen in a) and b) have been removed, only longer, deeper microcracks remain.

suggests some crystallographic influence; possibly, the long axis parallels the c-axis. Many of the "pimples" have a bright spot at their apex, which either indicates a sharp point or a different material, such as an impurity.

With increasing dissolution, cracks within a grain widen and the crack density changes, usually decreasing (cf. Fig. 4a, b, Fig. 3b, Fig. 3c). As dissolution occurs, the grinding/polishing induced microcracks widen with the shorter, more closely spaced microcracks progressibly impinging on surrounding neighbors resulting in mutual annihilation. With continued dissolution, the longer, more widely spaced cracks follow suit, leaving ultimately only the deepest cracks or newly exposed intragranular flaws as distinct surface features. As a consequence, the evolution of the roughness of an individual grain is complex. Initially the grain is very smooth. In early stages of dissolution modification, roughness progressive increases as the grinding/polishing induced microcracks widen. But with continued dissolution and associated crack widening, only the larger grinding/polishing microcracks and recently exposed pre-existing intragranular microcracks, holes or tubules will remain. In between these more widely spaced surface features are regions that are relatively smooth (see Fig. 3c). With continued dissolution, the remaining flaws widen but additional microcracks, holes and tubules are continually intersected by the free surface. The roughness is expected to approach an "equilibrium" roughness that reflects the density of intragranular dissolution "sites" and the rate of the annihilation by widening. The geometric details of the dissolution "sites" (i.e. spherical holes vs. cylindrical tubes vs planar cracks) together with crystallographic controls on dissolution rates will also influence the "equilibrium" roughness of a grain.

Progressive changes of surface roughness and morphology of individual grains are significant, but possibly of equal or even more importance with respect to fracture permeability are the changes of grain boundary widths. Initial apertures range typically from 0.1 to 1.0 μm. Upon reaction with the 0.1 N Na_2CO_3 solution, the aperture has increased to 2.5 μm to 5 μm, for a 0.4 N solution the range typically is from 7 μm to 16 μm, whereas for a 4.0 N solution the range is from 10 μm to 30 μm. All grain boundaries do not widen by the same amount, as indicated by typical ranges of apertures given (also see Fig 3c.) Furthermore, grain boundary widening decreases with distance away from the original outer surface. Significant widening appears to be restricted to one to two grain diameters

as shown in Figure 3c (see letter C) where a surface grain has become detached and the underlying grain boundary is exposed. An additional point to note is the crystallographic control on the shape of the widening microcrack, hole or tubule. The exact shape varies from grain to grain because of the difference in crystallographic orientation.

Tensile Fracture Surface

Dissolution induced changes of roughness and surface morphology differ in detail from that for polished surfaces because the tensile fractures lack the grinding/polishing surface features. Furthermore, a tensile fracture consists of both transgranular and intergranular fracture segments (Fig. 5a). The latter follow grain boundaries, hence have a significant initial microroughness. The transgranular segments, in contrast, are conchoidal in character exhibiting characteristic, low amplitude ripples and steps; these transgranular surfaces transect intragranular microcracks, holes and tubules.

Figure 5 shows stereo pairs of representative tensile fracture surfaces. Figure 5a corresponds to the unaltered surface; Figure 5b and 5c represent surfaces reacted, respectively, in 0.1N and 0.4N Na_2CO_3 solutions. Note the progressive roughening of grain boundaries as dissolution occurs at numerous holes or tubules located at grain boundaries. Transgranular surfaces also are modified significantly. Fracture surface markings become progressively subdued and holes and tubules widen. The latter features exhibit crystallographic control of shape (Fig. 6); if these holes or tubules are aligned, as along a healed microcrack, then with continued dissolution the neighboring holes interconnect, giving rise to channels of significant length and width within a grain (e.g. Fig. 5c).

Grain boundary widening is equally significant for tensile fracture surfaces as for polished surfaces, as one might anticipate. .The amount of grain boundary widening is similar for similar degrees of dissolution. Figure 7 shows representative grain boundaries widened by dissolution.

Pressure Solution Experiment

The results of the single experiment are not definitive, but there is a suggestion some pressure solution may have occurred. First, during the experiment, there was a continuous, but slow rate of shortening of the sample/piston assemble. Prior to loss of confining pressure, a total shortening of 5 μm had occurred (note: diameter of sand grains is about 100 μm). Examination with SEM of the polished Sioux Quartzite surface shows a number of surface features that appear to be produced by a concentrated load, as at a sand grain contact (Figure 8a). Figure 8b shows a close up view of one of these features. Note the flake-like piece adjacent the rather irregular depression. The flake could be correlative to a chip produced adjacent a concentrated load. The "ragged" character of the depression is of particular interest. Figure 8c shows another example of one of these surface features. The shallow depression to the side of the deeper region is of particular interest. These appear to be viable candidates for features produced by pressure solution, but additional studies are required for a more definitive identification. It is noted, however, the dimensions of these surface features is compatible with areas of contact of sand grains on the order of 100 m diameter. Furthermore, the depth of the depressions on the surface seem compatible with 5 μm of shortening by pressure solution.

DISCUSSION

The experiments clearly show the importance of structure defects, such as intragranular and intergranular microcracks, pores and tubules upon dissolution modification of surfaces. These features relate to the rocks structural history, its subsequent annealing or "healing" history (e.g. healed microcracks)

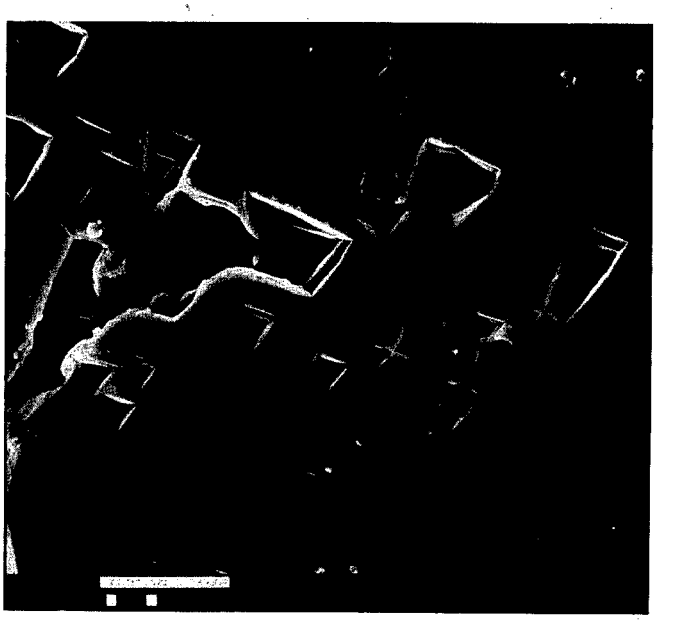

Figure 6. Crystallographic control of dissolution widening of pores and tubules along healed microcrack. Scale bar is 10 μm.

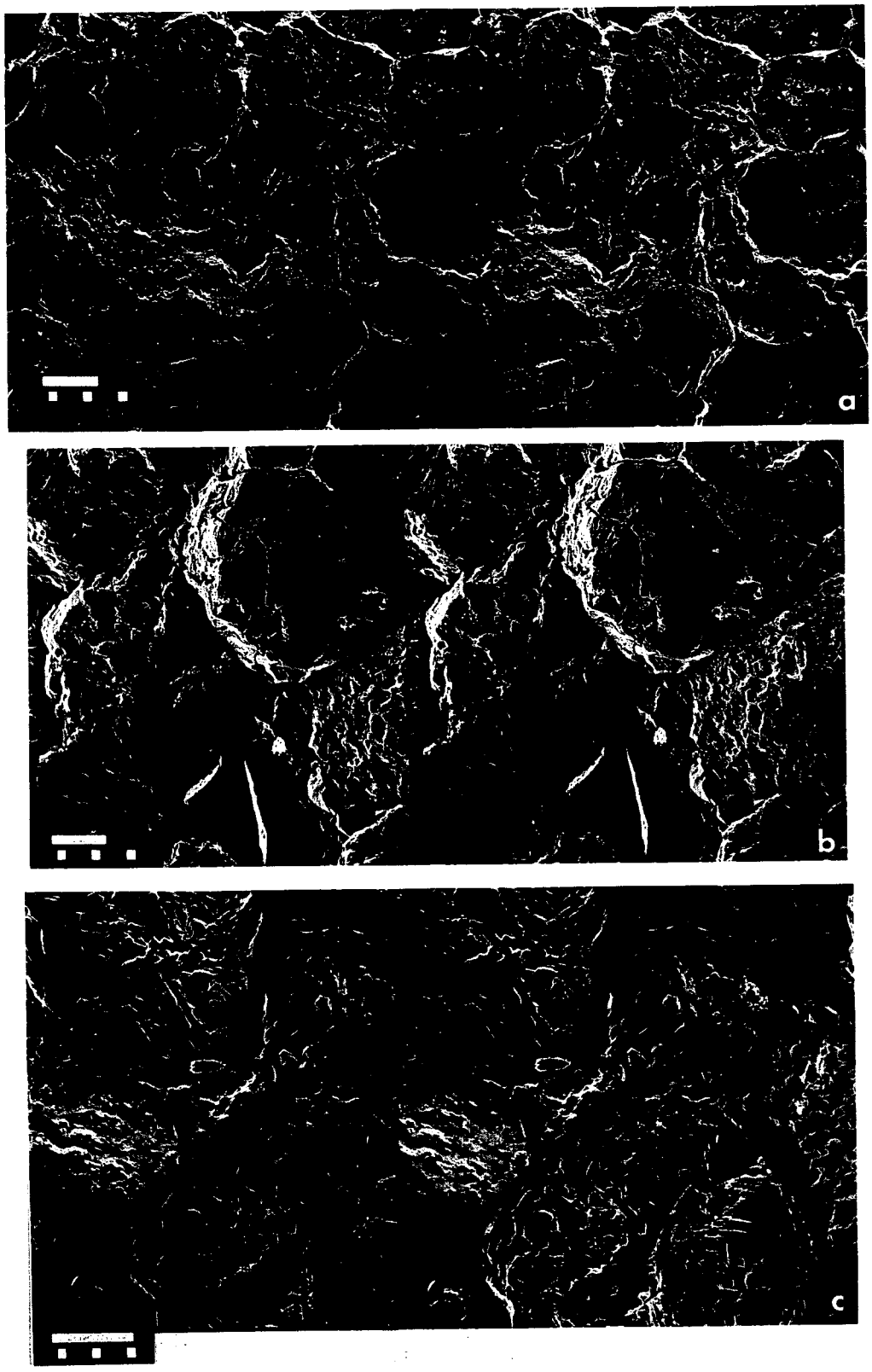

Figure 5. SEM stereo photographs showing progressive modification of surface morphology with increasing amount of dissolution. Initial surface is tensile fracture surface. Scale bar is 100 μ m. a) unaltered b) 0.1 N Na_2CO_3; c) 0.4 N Na_2CO_3.

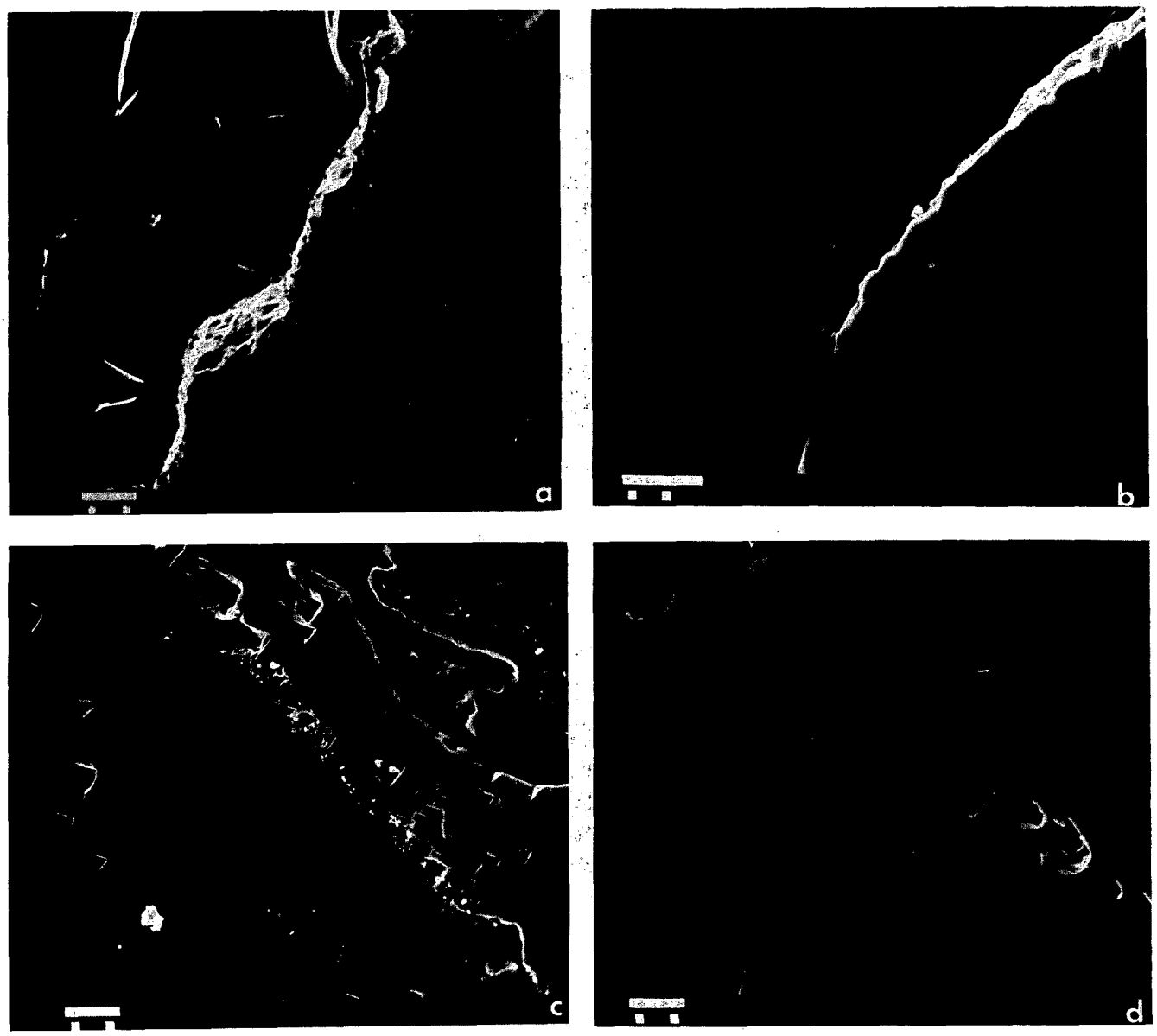

Figure 7. Widening of grain boundaries with progressively greater amounts of dissolution. a) distilled water; b) 0.05 N Na_2CO_3; c) 0.1 N Na_2CO_3, d) 0.3 N Na_2CO_3. Scale bar is 10 μm.

and the effects of sample preparation (e.g. grinding/polishing induced cracks and thermal cracks). Emphasize is placed on brittle deformation features, but plastic deformation features (e.g. dislocations) may be significant in certain cases as will be discussed briefly subsequently. One particularly important result the experiments emphasize are the effects of sample preparation induced structural defects, most specificly grinding /polishing microcracks. As shown, these play a dominant role, at least in the early phase of the evolution of the surface undergoing dissolution. This is significant because a large portion of "fracture" permeability experiments to study effects of stress variation have utilized contacting saw cut or abraded saw cut surfaces. In these cases, the size of the preparation induced cracks would be larger than in "polished" surfaces used in the experiments reported here. One would expect, as a consequence, observed permeability changes due to dissolution fluid/rock interactions would strongly reflect the influence of these structural defects. This would complicate the application of the results to the case of a "natural" fracture. Such a difficulty is not as apparent, however,

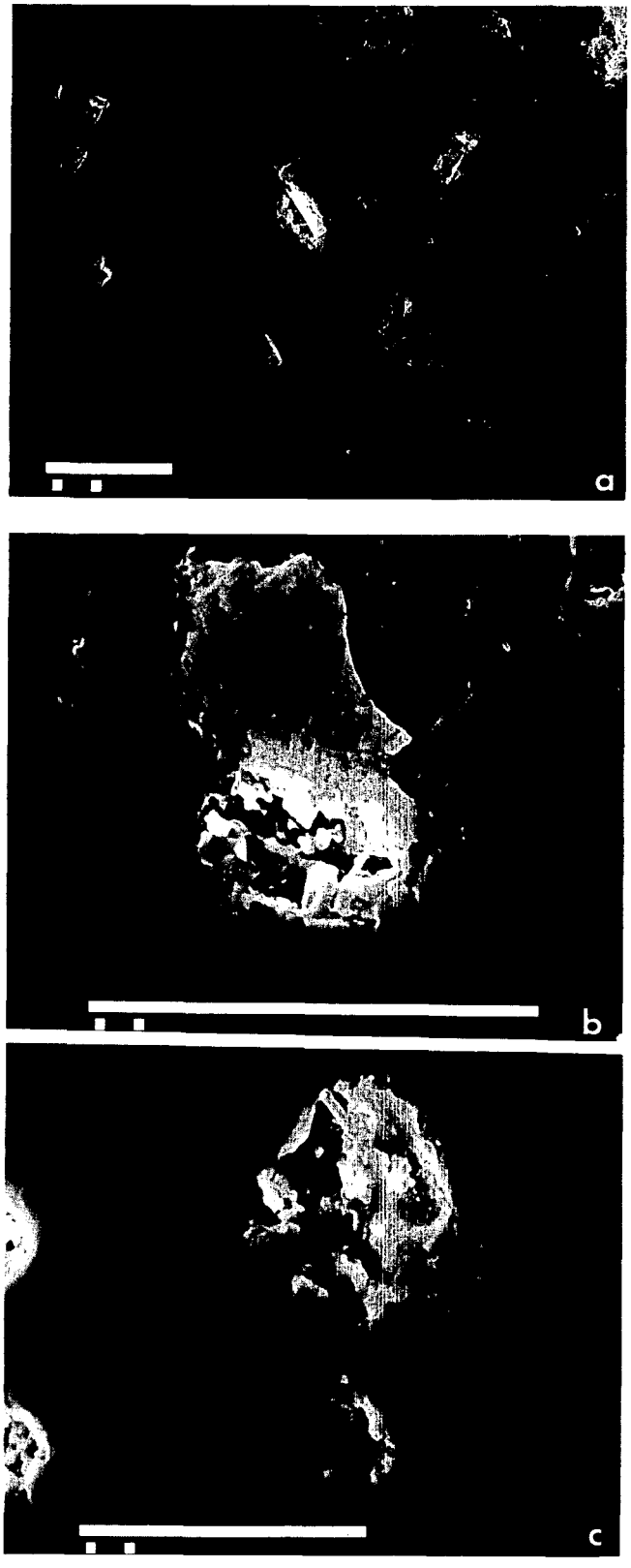

Figure 8. SEM photographs of possible pressure solution features produced by indenting quartz sand grains. Scale bar is 10 μm.

with respect to assessing the effects of normal stress variation (achemical effects) on permeability. Consequently the choice of the "fracture" surface must be made carefully if the chemical effects are to be studied.

The change of cracks and pores into geometric forms bounded by crystallographic planes reflects the action of the dissolution medium and difference of dissolution susceptibility in different crystallographic directions. Sufficient experimental data exists on quartz growth and dissolution to provide insight into the basic aspects of this effect. Ballman and Landise (1963) provide a summary of hydrothermal growth of quartz in alkaline solutions (aqueous NaOH and Na_2CO_3). They show the rate of crystal growth is dependent on crystallographic directions, as shown in Figure 9. In terms of specific crystallograhic planes, note that the relative rates of growth are $\{0001\} > \{01\bar{1}1\} > \{1\bar{1}01\} > \{10\bar{1}0\}$. Crystal growth rates are useful when considering dissolution of quartz, because the relative rates of dissolution in different crystallographic directions closely mirrors that of growth. The slow growing surfaces are also the slower dissolving surfaces. Frondel (1962) demonstrates this in his summary of other workers studies of quartz itching and dissolution. Figure 10 shows how a quartz sphere changes shape upon extensive dissolution. The rate of solution is greatest in the direction of the c-axis and a minimum along an a-axis (the X axis in the orthogonal axis system shown in Figure 9a). It is not uncommon for dissolution rates to be 5 times greater than corresponding growth rates (Mullin, 1972). In the case of quartz, the ratio of the rate of dissolution parallel to the c-axis to that normal to a hexagonal prism $\{1010\}$ is about 100:1.

Comparison of dissolution features produced in these experiments with published results for chemical etching of quartz (to reveal dislocations and other deformation substructures, see Wegner and Christie, 1983 for comprehensive review) indicates that most of the dissolution features developed do not appear to be related to dislocations. They do not have the shapes characteristic of dislocation etch pits. The only exception to this might be the features referred to as tubules might in part be deep etch tubes (Frondel, 1962); this seems unlikely, however, since a larger number of pores and tubules are observed intersecting unaltered transgranular fracture surfaces(Figure 1). Nevertheless, dislocations are known to exist in the grains because of the occurrence of deformation lamalle, hence one might expect to observe associated etch pits, provided the Na_2CO_3 solution acts as a suitable solvent for preferential etching of dislocations.

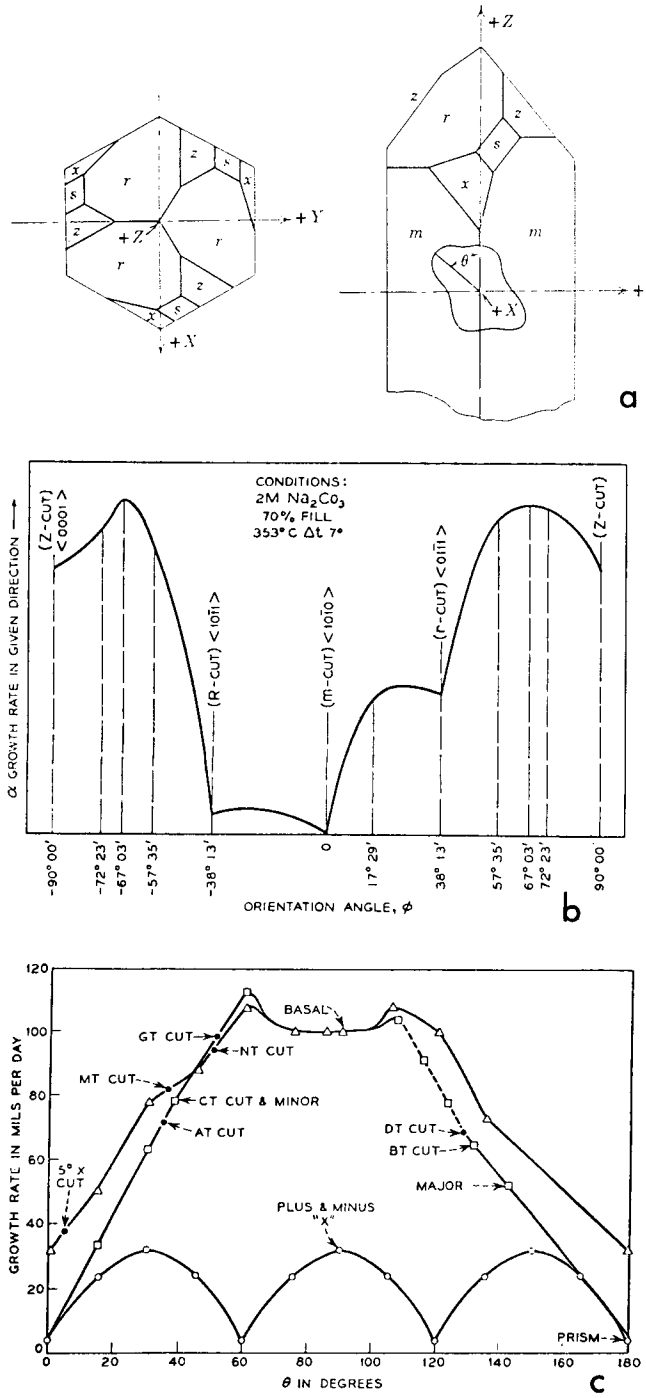

Figure 9. Rate of growth of quartz in NaOH and Na_2CO_3 solutions as a function of crystallographic direction. a) orthogonal reference axis; b) growth of quartz in Na_2CO_3 solution for seed crystals cut with normal in Y-Z plane, $\theta = 0°$ for normal parallel to c-axis; c) growth rates of quartz in NaOH solutions, curve 1 is for seeds cut with normal in Y-Z plane, curve 2 is for seeds cut with normal in X-Y plane (from Ballman and Landise, 1963).

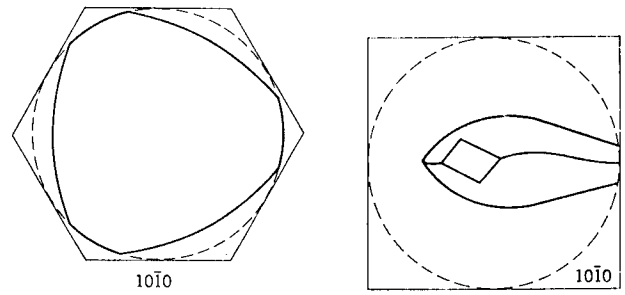

Figure 10. Relative rates of dissolution of quartz as a function of crystallographic direction as shown by shape changes of quartz sphere subjected to long-continued attack by HF. Dotted line shows the outline of the original sphere; inner solid lines show the outline of dissolution modified shape. Left view is along c-axis; right view is perpendicular to a hexagonal prism face (after Frondel, 1962).

Grain boundary widening is a prominent dissolution change. This reflects the existence of the significant numbers of grain boundary pores and cracks, the rough character of the grain boundary and the common occurrence of holes or tubules at the grain boundaries and in adjacent solid; all these act as nuclei of dissolution. The widening of the grain boundaries produces additional interconnected flow channels, hence will increase fracture permeability, all other things remaining constant. The amount of widening across any specific grain boundary should reflect the relative crystallographic orientations of the juxtaposed grains; however, differences in the microdefects in the respective grain surfaces may modified this effect.

As noted earlier, the widening of grain boundaries is observed to be restricted to a depth of about one or two grain diameters. Transport of the dissolved silica outward from the deeper regions of the grain boundaries is believed to be predominatly by diffusion, with convective transport being minimal in the narrow capsules. If fluid flow occurred, the depth of grain boundary widening is expected to increase, hence the effects of these cracks on fracture permeability should be even greater. Channeling effects would also be anticipated as a consequence of the dissolution rate depending upon the flow rate (fluid undersaturated with respect to solid).

The effective stress is zero in the dissolution experiments, hence care must be exercised in extrapolating these results to the case of a fracture subjected to a nonzero

effective normal stress. Nevertheless, the results suggest several ways in which dissolution may modify fracture permeability. If dissolution increases the over all roughness of the fracture surface, then the effective hydraulic aperture is expected to increase. The widening of grain boundaries may be of special importance; they may represent a significant increase of fracture aperture, plus their closure may be less dependent upon changes of stress normal to the fracture. Widening of grain boundaries, however, will remove lateral restraints of load bearing asperities resulting in an increase of the fractures' elastic and inelastic compliance. For example, widening of grain boundaries may permit eccentrically loaded grains to rotation, hence affecting fracture compliance. Dissolution also changes the size and shape distribution of asperities on grains. The experiments indicate the roughness of individual grains increases on the average, as a consequence, the compliance of an individual grain is expected to increase. This in turn will result in a stronger stress dependence of the fracture permeability. Future experiments measuring dissolution induced changes of the fracture permeability of the Sioux Quartzite, should provide addition insights into the tentative hypotheses.

ACKNOWLEDGEMENTS

This research has been supported by the office of Basic Energy Sciences, Division of Engineering, Mathematics and Geosciences, U.S. Department of Energy, contract no. DE-AS05-79ER10361. Dr. Steve Fritz provided the chemical analysis of the Sioux Quartzite. Ken Wilks and Richard Borkowski assisted with some of the experiments.

REFERENCES

Ballman, A.A. and Landise, R.A., 1963, Hydrothermal growth of crystals: in Gilman, J. (ed), The Art and Science of Growing Crystals, chapter 13, Wiley and Sons.

Friedman, M. and Bur, T.R., 1974, Investigations of the relations among residual strain, fabric, fracture and ultrasonic attenuation and velocity in rocks: International Journal of Rock Mechanics and Mining Science and Geomechanics Abstracts, v. 11, p. 221-234.

Friedman, M. and Johnson, Brann, 1978, Thermal cracks in unconfined Sioux Quartzite: Proceedings of 19th U.S. Rock Mechanics Symposium, May 1-3, 1978, Stateline, Nevada, p. 423-430.

Frondel, C., 1962, Dana's System of Mineralogy, 7th ed., v. III: Silica Minerals, Wiley and Sons, N.Y., N.Y., 334p.

Johnson, Brann, Gangi, A.F., and Handin, J., 1978, Thermal cracking of rock subjected to slow, uniform temperature changes: Proceedings of 19th U.S. Rock Mechanics Symposium, May 1-3, 1978, Stateline, Nevada, p. 259-267.

Krech, W.N., Henderson, F.A., and Kjelmstad, K.E., 1974, A standard rock suite for rapid exacation research: U.S. Bureau of Mines, Report of Investigations, no. 7865, 29p.

Mullin, J.W., 1972, Crystallisation, CRC Press, 2nd ed., 479p.

Shirey, S.B., Simmons, G. and Padovani, E.R., 1980, Angular, oriented microtubes in metamorphic plagioclase: Geology, v. 8, p. 240-244.

Wegner, M.W., and Christie, J.M., 1983, Chemical etching of deformation substructures in quartz: Physics and Chemistry of Minerals, v. 9, p. 67-78.

DISCLAIMER

This report was prepared as an account of work sponsored by an agency of the United States Government. Neither the United States Government nor any agency thereof, nor any of their employees, makes any warranty, express or implied, or assumes any legal liability or responsibility for the accuracy, completeness, or usefulness of any information, apparatus, product, or process disclosed, or represents that its use would not infringe privately owned rights. Reference herein to any specific commercial product, process, or service by trade name, trademark, manufacturer, or otherwise does not necessarily constitute or imply its endorsement, recommendation, or favoring by the United States Government or any agency thereof. The views and opinions of authors expressed herein do not necessarily state or reflect those of the United States Government or any agency thereof.